New Directions in Mechanics and Cooling for Pixel Detectors

William O. Miller, Innovative Technologies International (iTi)

Wei Shih, Allcomp Inc.

Pixel Detector Cooling Issues

Pixels are becoming an essential part of precision tracking for charged-particle detection systems. Their growth in size has been phenomenal; presently being driven by needs of the Large Hadron Collider ATLAS Detector Program, where the Semiconductor Tracker (SCT) and the Pixel Detector, occupy a combined volume of nominally $18m^3$. As originally configured the ATLAS Pixel Detector active area was $2.3m^2$, requiring a cooling capacity of 14kW [1].

Recent advancements in pixel technology have been focused on achieving the LHC physics requirements with respect to precision tracking, and radiation damage resistance. Radiation damage is of concern because of the detector module's close proximity to the interaction point. The ATLAS Pixel detector provides a robust pattern recognition capability, coupled with excellent vertex capability. With their high performance come also unique requirements for cooling, with heat dissipation being localized at the integrated pixel electronics, which are distributed throughout the detector space. This attribute is in sharp contrast to the silicon strip detectors. Hence, achieving efficient cooling and low mass pixel module supports not only present interesting and challenging problems, but on-going ones as well.

The ATLAS Pixel Detector [1] material average *unit radiation length* budget was originally projected to be as low as 4.2% at η of zero. This amounts to 1.4% X_o per layer, where X_o represents the percentage radiation length. It now stands at 2.0% [2] per layer, with a substantial increase at $\eta \sim 2$. This increased mass, largely structural and cooling system components, has a deleterious effect on the ATLAS electromagnetic calorimeter and on track finding in the Inner Detector [1]. In general, this performance degradation provides impetus to developing new structures, new materials, and new approaches and concepts.

It is our objective to tackle the detector mass problem by simultaneously addressing structural and cooling aspects, striving for a new integrated approach with less complexity and fewer components.

ATLAS staff has made a significant performance contribution by introducing forced-convective, cooling using a two-phase evaporative cooling medium. However, a circulating, convective heat transport system tends to bring with it system complexities, and stability issues. Our innovation is to solve these problems by applying heat-pipe technology, a passive heat transfer device. Heat-pipes, with a two-phase fluid in a completely closed system, are capable of extracting and transporting heat over long distances, with a phenomenally high effectivity. Compared with copper on heat transport basis, heat-pipes would be 1000 times better. This

technology has advanced to the point (>10^6 hours operational life) where it is currently used as a heat spreader in laptop computers. Our technical objective is to produce a carbon-carbon (C-C) heat-pipe with a low effective $\%X_o$, by drawing upon the present tech-base. Our proposed concept will solve not only high-energy-physics (HEP) detector cooling problems, but very high temperature aerospace applications as well.

By our approach of passively transferring heat, we eliminate the complex pressure regulation system found necessary to control the ATLAS Pixel Detector and SCT two-phase coolant system. Furthermore, we substantially reduce the large array of cooling tubes entering and leaving the tracking volume, and their associated plumbing connections. Our proposed simplification is projected to greatly increase system wide-reliability, which is extremely important in the maintenance of largely inaccessible equipment. In the final step, we look carefully at how the cooling system is integrated with the detector, seeking an innovative structural approach that will noticeably lower mass further.

Pixel Detector Thermal Issues

Pixel electronics uniformly distribute the heat, creating a heat flux as high as $0.8W/cm^2$ at the module interface and much higher still at the cooling tube interface, which is directly beneath the modules. Highly integrated cooling and support structures, which draw upon specialized composite materials and structures, have evolved to remove this heat. In addition, much development has gone into selecting the appropriate coolant to remove this thermal load. Both the ATLAS Pixel Detector and SCT Detector collaborations have settled on an evaporative fluorinert coolant C_3F_8 to accomplish this objective. It becomes our goal to draw upon this technical base, while substantially improving the thermal performance and reducing system mass.

Specific Pixel Barrel Support Issues

ATLAS pixels rely on a stave configuration for module supports in the barrel region; staves comprising an integral cooling tube, coolant tube housing, thermal grease and with the primary support provided by a support shell. A solid model of the outer layer extracted from the ATLAS Pixel Detector is shown Figure 1. The ATLAS stave is a composite structure, requiring discrete supports over its 800mm span, to limit gravitational sag.

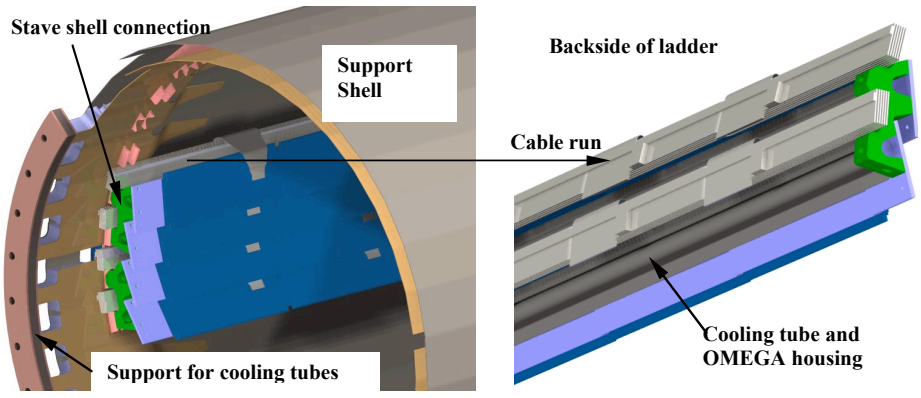

Figure 1: Close-up of end view for the ATLAS Pixel Detector Layer L2, including an illustration of the backside of the ladder. Circular arc on shell end provides a support and strain relief for terminating the cooling tubes.

Figure 2 illustrates a portion of the array of the return cooling lines (C_3F_8 vapor) from the barrel region. There is one inlet and one return line for a pair of staves. This amounts to 56 inlets and 56 returns for the barrel region alone.

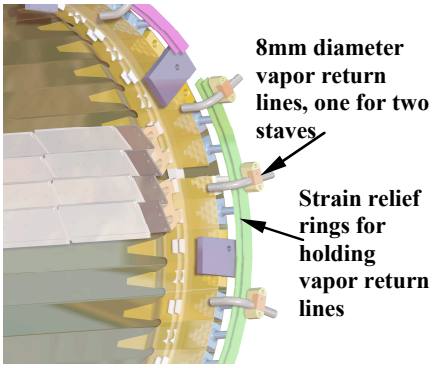

Figure 2: Illustration of the plumbing lines emanating from the Pixel Detector Barrel.

Figure 3 depicts a calculation of the material radiation length for the ATLAS Pixel Detector, for all three layers, including modules. At normal incidence the ladders (stave plus modules) is roughly 2% per layer. The module with flex hybrid is nominally 0.86%, and the mechanical support 1.28%. At an □ of 1.9, one can see that the combined radiation length increases to 25%. This serious material issue in the forward region arises from the extra mass associated with the coolant tube routing, coolant tube connections, and heavy shell flanges at each end.

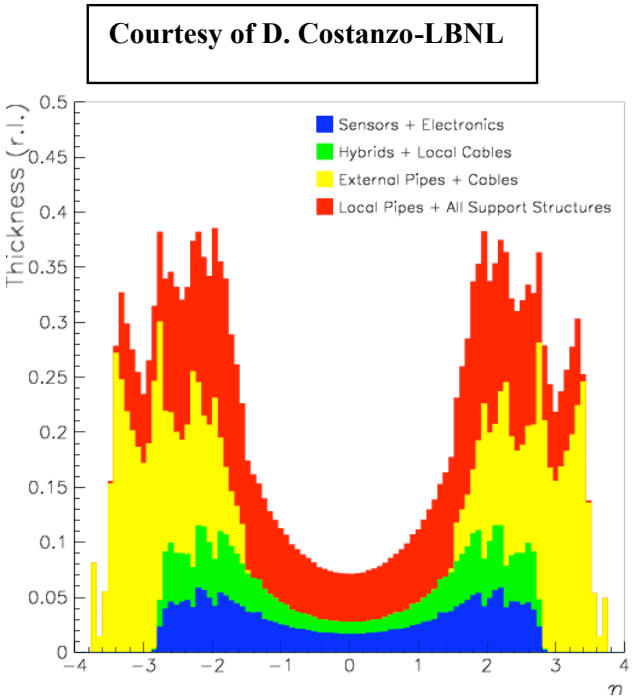

Figure 3: Thickness in unit radiation lengths for the ATLAS Pixel Detector Barrel Elements as a function of □. Value displayed represents the total unit radiation length for layers including the outer support frame and end cone support components.

Our objective is to focus on developing a more innovative, mass efficient highly integrated structure and cooling concept.

New Directions for Pixel Detector Mechanics and Cooling

Barrel Frame Structure for a Heat-pipe Concept

Our objective is to achieve a high performance, efficient detector concept by integrating heat-pipes with a pixel module support structure. To gain an appreciation of the pipe structural size we performed preliminary calculations on three basic geometries:

a. Tube bundle, connected by circumferential rings
b. Tube with attached plate, bundled in same fashion as (a)
c. Tube/plate shell-like structure

In each case the concept is based on an array of 6mm mean diameter tubes, with a 0.3mm wall on a 100mm radius, 38 tubes in all. For case (a) and (b) the tubes were structurally connected circumferentially with thin rings (0.45mm thickness, radial depth 6mm) at 6-equal spaces. This array was rigidly *fixed* at the two ends[1].

For case (a), we find the gravitational sag of the bundle to be 33.8□m, Figure 4; whereas, an equivalent closed-form analytic solution gave 38□m^2, based on the tube moment of inertia only. It is clear that a simple tube bundle alone would provide inadequate support for the modules.

The FEA of case (b) yielded maximum gravity sag of nominally 28.3□m, Figure 5. This geometry has a flat strip added to the tube, simulating the module mounting structure, ala the ATLAS barrel concept. The FE model (b) was obtained by adding a 14mm wide by 1mm thick plate tangent to the outer surface of the tube. The combined moment of inertia is large whenever this plate side[3] becomes normal, or nearly normal to the direction of gravity. It is this substantial increase in moment of inertia, in a portion of the array, which prevents the sag from increasing in direct proportion to the increased mass. The mass of the system is now weighs 1.027kg, as opposed to 0.31kg for (a).

[1] Convenient boundary condition imposing maximum restraint. Actual supports are more akin to simple supports, with 5 times greater deflection.
[2] Note: it is apparent that tube bundle does not sag as a group about the neutral axis (center of tube array).
[3] Ratio of moment inertia of the plate in the x and y direction respectively is $\frac{I_{px}}{I_{py}} = 195.9$.

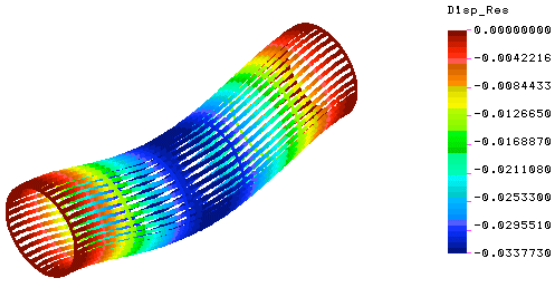

Figure 4: FE solution for gravity sag of a 38-tube bundle joined with 6-rings equally spaced over the 800mm length with a mean diameter of 200mm. Each tube has a mean diameter of 6mm with a 0.3mm wall thickness. The rings have a thickness of 0.45mm. Both materials have an isotropic value of Young's Modulus equal to 103.4GPa (15Msi). Maximum sag at the center is 33.8microns. Weight of one tube is 6 g's, and the overall weight of the structure is 0.31kgs.

Besides weighing 1.027kg, the radiation length is 0.52%[4] (tubes without the module support equaled 0.16%). It is clear that the gravity sag cannot be reduced to acceptable levels, at least for this example, without a more efficient structure.

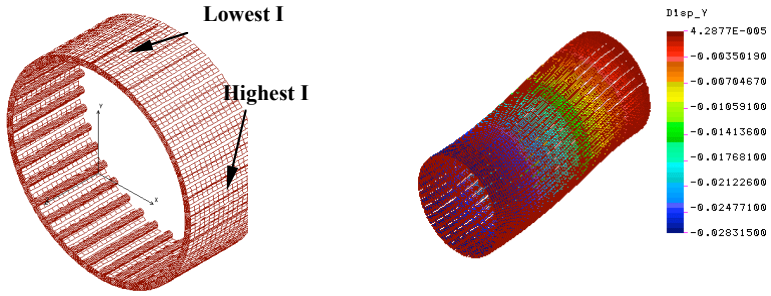

Figure 5: FE model of stave with a flat strip, 14mm by 1mm, as a heat spreader mounted on a coolant tube with a mean diameter of 6mm with a 0.3mm wall thickness. The geometry of the tube bundle array is the same as shown Figure 4. The peak gravitational sag has now been reduced to 8.33μm. Only half of the FE model is shown, with the split at the mid plane.

In ATLAS, the solution for overcoming sag was to mount the support rings to an external shell (clamshell). A continuous shell with 100mm radius (0.45mm thickness) would sag only 0.138μm under its own weight. Theoretically, this shell could support 100 times its weight before sagging 13.8μm. The shell weighs only 0.385kg and it can easily support 4.2kg, corresponding to 38 staves at 110g/stave. The shell only adds a radiation length of 0.18% without any form of light weighting (normalizing at the 100mm radius).

For case (c), we consider a shell-like structure composed of tubes and plates, ala CMS, for a pixel barrel concept. The detector modules are mounted on a structure composed of longitudinal (light weighted) flat segments joined at the segment edges by cooling tubes. The shell-like

[4] Mass averaged over the surface of a cylinder with a 100mm radius. As a reference, this value is close to the original ATLAS design goal.

structure creates an up-down pattern with regards to module placement, as the tube attachment alternate from inside to outside.

Figure 6 illustrates results for case (c), using comparable dimensions to (a) and (b). No attempt was made in the FEA to simulate steps that may be taken to lightweight the longitudinal strips in area directly beneath the modules.

The deflection of this composite structure is noticeably reduced over the previous example. Here the deflection is just 2.4μm. The basic structure, including our choice of tube geometry for the proposed heat-pipe, is nominally 0.7kg; this is largely a result of choosing 0.45mm thickness for the web segments and the 6mm diameter tube geometry. Further structural analysis and a 1st order thermal study is justified to support these arbitrary selections. Adding the module and cable mass would triple the mass, but still with an acceptable 7.2μm sag. We notice from Figure 6 that most of the sag will occur in the upper region.

There is obvious structural merit to this concept, but additional work is needed to evaluate the thermal strains that may result. It is clear that the module heat must now flow to the edge of the heat spreader, not to the heat-pipe directly beneath the heat source. In a separate study, our approach to this issue would be to investigate using TPG[5] material sandwiched with high modulus graphite fibers.

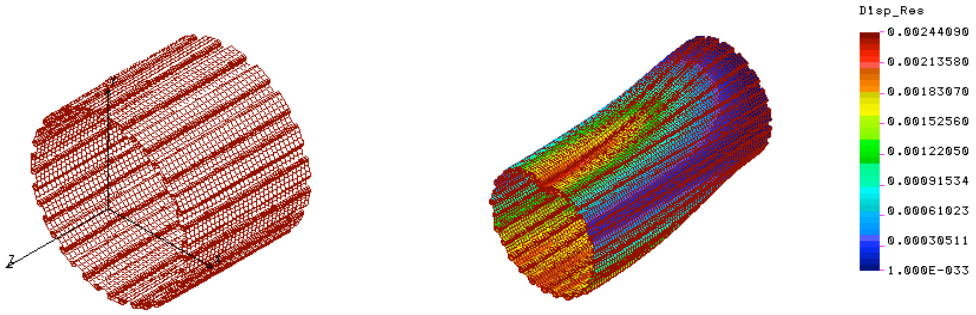

Figure 6: FE model of barrel stave support concept fashioned after a concept extracted from CMS Pixel Detector information. The model is a simple extension of the 38-tube concept (a) in Figure 4. Peak central deflection of the shell-like structure is 2.44μm.

Summary of Barrel/Heat-pipe Construction Options

We have briefly evaluated structural merits of three geometries for implementing the heat-pipe cooling. Case (c) appears to offer best potential for lower structural mass, but more analysis is needed to clarify this point. Both concepts (b) and (c) are suited to our innovative cooling system proposal. To illustrate our proposed innovation we proceed with an adaptation to the ATLAS Pixel Detector. More is known about this design; consequently, for our proposal it is possible to develop a 1st order performance comparison. We propose to look into the CMS structural design option carefully, with the objective of further reducing structural mass.

[5] TPG-thermally conductive pyrolytic graphite

Detector Cooling with Heat Pipes

The ATLAS Pixel Detector cooling relies on an evaporative fluorinert fluid, C_3F_8 (92.8W for 1g/s circulated), for a performance advantage over non-phase change liquids. Extensive development has gone into this concept. Nonetheless, system wide issues for adapting this concept to a very large array of coolant tubes persist.

As presently configured for the ATLAS Pixel Detector, it requires 80 inlet and return lines, approximately split between detector ends, to circulate fluid through the barrel and two disk regions. In addition, to control module temperature, the evaporative system requires a pressure regulator on both the inlet and exit of the sector or stave. Successful implementation of the C_3F_8 is anticipated. Nonetheless, one should be mindful of the potential reliability problems that may be encountered in operating and maintaining such a complex flow system.

Coolant plumbing and interconnections in the tracking volume, account for much of the cited mass. In addition, the various diameters of the numerous vapor-return lines are substantial. One can argue that coolant % X_o has been minimized, but it is rather clear that this accomplishment comes at a substantial penalty, both added material and added complexity. Our innovation will eliminate these disadvantages, while retaining the benefits of an evaporative cooling system (C_3F_8).

Our approach is to use a heat-pipe concept to remove and transfer heat to a region more amenable for removal. The module heat is transferred to the end of the heat-pipe, where the heat is removed by a cold condensing section. A heat-pipe is an entirely sealed chamber, filled with a small amount of a two-phase fluid. The chamber is first evacuated before charging with the fluid, thus the chamber pressure is governed by the fluid vapor pressure. Fluid evaporation picks-up heat from the chamber wall over the length of the evaporation section, and gives-up the heat by fluid condensation in condensing section. In our design approach, we have eliminated the adiabatic section between the evaporation and condensing sections, since it is not needed, making the concept more compact.

The heat-pipe uses a wick to transport the liquid to the heated region, where the evaporating fluid creates a pressure gradient, forcing the fluid vapor back to the condensing section. A central core provides space for the returning vapor. This mechanism, optimum for transporting heat, provides two-phase heat transfer capabilities from one hundred to a thousand times the thermal conductivity of copper.

Fundamental design parameters in the wick structure are pore size to produce capillary pressure, and permeability to lower pressure drop for liquid transport. An adequate vapor core (cross-sectional flow area) is needed to limit vapor velocities.

Initially, we plan to place the evaporation section of the heat-pipe directly beneath the module, thereby minimizing the structure's thermal gradient. A condensing section will be placed at each stave end. However, our initial prototype will be a heat-pipe equal to _ of a stave; thus, making the barrel plane of symmetry (Z=0) as a convenient thermal boundary condition. Our design goal for extracted heat in this half stave length is set at 55W, the maximum power point for ATLAS testing. In the final design concept, the condensing section at the end of the stave

transfers this heat to the C_3F_8 evaporative fluid. This connection we intend to make through highly conductive[6] composite materials.

There will be no need for fluid interconnections between adjacent heat-pipes as now exist for the ATLAS pixel barrel. This equates to eliminating the metallic, thermal expansion bellows between adjacent staves, a definite improvement to dimensional stability.

Another major advantage is reducing the number pipes entering and leaving the detector space to two entering and two leaving per barrel end. This number may readily be increased to satisfy a request for redundancy. The modularity of the barrel section is actually improved, since in our concept one heat-pipe serves a stave, whereas it seems popular to interconnect two adjacent staves in series.

1.1.1 Candidate Heat-pipe Fluids and Heat-pipe Sizing

The proposed heat-pipe is a sealed, cylindrical tube, although flat heat-pipes are common. It is conceivable that in a full system detector design, composed of both barrels and disks, this attractive feature could be exploited to advantage (e.g., disks).

There are many factors to consider when designing a heat-pipe, compatibility of materials, operating temperature, diameter, power limitations (installed volume), thermal resistance, and operating orientation. Two options for this application, the material and fluid for example, are somewhat limited. In particular, materials must be the chosen to minimize $\%X_0$, and the evaporation temperature is set by the need to hold a module temperature $\leq -10°C$. We add a desirable attribute, i.e., a low to moderate pressure heat-pipe, over the range of temperatures expected. Invariably, the coolant containment and module support are integrated. Strain in the coolant containment can couple to the pixel modules support, posing a thermal stability issue. We wish to mitigate this effect through a choice of heat-pipe working fluid. In this regard, the C_3F_8 ATLAS is a high-pressure system and the stave and sectors had to be structurally qualified to 10bar. Structural integrity was achieved and demonstrated, but at the expense of additional material.

Table 1 and Table 2 list a subset of fluid properties important to configuring and sizing a heat-pipe. In the discussion to follow, we will present the rationale for choosing these particular fluids for this application. We see next that the figure of merit term in Table 1 is highly useful in picking a fluid candidate.

Fluid is supplied throughout the heat-pipe evaporation section via a wick. A sampling of common wick structures is metallic screens, porous media (sintered metal, carbon and graphite foam, etc.), and axial grooves. Grooving the wall circumferentially is also an option; in this case, a *slab* porous wick is used to feed the grooves. Capillary pressure developed in these wick structures provides the driving force (pressure) to overcome the flow resistance. Frequently, this capillary limit sets the design configuration in a heat-pipe application. As an observation, pressure drop in the ATLAS system was the driving factor behind the selection of the C_3F_8, after the decision was made to use a two-phase fluid.

---

[6] TPG sandwich, composed of high K carbon-carbon and 1300 W/mK pyrolytic graphite. TPG material was introduced earlier by W.O. Miller to ATLAS staff, as a means of eliminating thermal runaway in radiation damaged silicon strip detectors

To the first order the capillary pressure is given by:

$\Delta P_c = \frac{2\sigma}{r_c}$; where, σ and r_c correspond to the fluid surface tension and the wick pore radius. Small *equivalent* pore radii and high fluid surface tension produce high capillary pumping pressure. Too small pore radius will impact the wick design. It will lower material permeability, which causes increased pressure drop in the wick. Through a suitable balance between wick permeability and pore radii, we are able to configure a very high thermal performance system.

The capillary pressure must overcome three pressure terms. These being:

a. ΔP_e: pressure drop to supply the fluid to the evaporator region, and

b. ΔP_v: vapor core pressure drop to return the fluid to the condenser, and

c. ΔP_h: hydrostatic pressure term to offset changes in elevation between the evaporator and condenser region. Hydrostatic pressure is produced in inclined heat-pipes. For barrel region, the heat-pipe would be horizontal, so the only component is a normal hydrostatic pressure, a term proportional to the diameter of the pipe. These terms are also found in ATLAS C_3F_8 system.

The *capillary limit* is given by:

$(\Delta P_c)_{\max} \geq \Delta P_e + \Delta P_v + \Delta P_h$. Aside from these pressure drop terms, the pipe must be sized to assure against sonic flow of the vapor and boiling in the wick structure. These are referred to as the *sonic flow and boiling limits.* A potential for sonic flow in the return line for ATLAS was also a consideration: it set the vapor return line sizes within the detector space and contributed heavily to the switching from C_4F_{10} to C_3F_8 in ATLAS.

We made a first cut at fluid candidates suitable for HEP detector applications. Ammonia, a very common organic refrigerant performs well. It will be our first choice, because of its distinct performance advantages. However, we know little about the fluid behavior in a radiation environment, consequently these tests need to be run. Next are hydrocarbons, Methanol and Isobutane. Lower performance candidates would be from the halogen and fluorinert families, R11 and R12, and C_4F_{10} and C_3F_8 respectively.

Methanol is well documented in heat-pipe applications, whereas Isobutane is less common. Isobutane was planned and successfully tested in a thermo-siphon, evaporative fluid concept for the SSC[7] silicon tracker. Development of this system was curtailed with the SSC project. A negative factor was that the concept employed an open vapor concept that required all the components to be compatible with the Isobutane.

The fluorinert fluids have been radiation tested for the ATLAS application and found to be entirely acceptable. The hydrocarbon fluid candidates are also radiation resistant. Testing of the Isobutane was performed at LANL for the SSC project. Strip detectors were immersed in Isobutane and irradiated with a cobalt source at University of California at Santa Cruz. Leakage-current testing of the strips before and after irradiation produced no discernible effect.

[7] Super Conducting Super Collider (SSC) silicon tracker program at Los Alamos National Laboratory, W.O. Miller and other key LANL staff members.

Refrigerants 11 and 12 provide a low-pressure option. Unfortunately, these fluids contain chlorine, and consequently they largely have been eliminated from industrial use. The disassociated chlorine radical from R11 or R12 damages the earth's ozone layer.

Table 1: Thermo-physical Properties for Selected Fluids for Potential Heat-pipe Application

Liquid	M_w g/mol	Latent Heat λ (kJ/kg)	Boiling Point T_{sat} (°C)	Vapor Pressure[a] (bar)	Density[a] ρ_l (kg/m^3)	Viscosity[a] μ_l (μPa s)	Surface Tension[a] σ (N/m)	Figure of merit[a] (kW/cm^2) $\frac{\rho_l \sigma \lambda}{\mu_l}$
Ammonia-NH_3	17.03	1296.2	-33.3	2.91	652.3	196.8	0.029	12460
Methanol-CH_3OH	32.04	1218	64.7	0.021	819.2	945	0.0263	2772
Isobutane-C_4H_{10}	58.13	364.6	-11.7	1.08	592.2	288.0	0.0167	1252
Refrig. 11-CCl_3F	137.4	193.2	23.7	0.26	1556.5	636.1	0.0224	1059
Refrig. 12-CCl_2F_2	120.9	157.6	-29.8	2.18	1427.1	287.5	0.013(?)	1017
Fluorinert- C_4F_{10}	238	99.5	-2.0	0.725	1634.5	621.1	.0074	19.4
Fluorinert- C_3F_8	188.2	92.8	-36.7	2.95	1502	216.7	.0043	27.7

[a] **Properties for -10°C**

At 25°C, the vapor pressure in an ammonia heat-pipe would be 10bar whereas at -10°C, the vapor pressure is 2.9bar. This pressure change should produce limited structural changes at the module level, assuming a suitably designed support. The Methanol fluid is a low-pressure option, but its lower vapor density will result in increased pressure drop in the returning vapor. To compare the performance of these fluids we made a first order design calculation using groove wick geometry.

Table 2: Selected Properties for Candidate Fluids for Heat-pipe Application

Liquid	Critical Temperature (°C)	Critical Pressure (bar)	Vapor Pressure (bar) @ 25°C	Liquid Thermal Conductivity (W/mK) @ -10°C
Ammonia-NH_3	132.2	112.8	10	0.591
Methanol-CH_3OH	239.7	81.0	0.2	0.206
Isobutane-C_4H_{10}	134.4	36.4	3.5	0.111
Refrig. 11-CCl_3F	198.0	44.1	1.1	0.098
Refrig. 12-CCl_2F_2	112.0	41.4	6.5	0.079
Fluorinert- C_4F_{10}	113.2	23.3	2.7	0.048
Fluorinert- C_3F_8	71.9	26.8	9.7	0.049

1.1.2 C-C Heat-pipe Calculations

The design point used to size the heat-pipe concept is for half of a stave length. The case chosen is a 400mm long evaporator section, with a 40mm condensing section. Of the wick geometries shown in Figure 7, we choose a groove wick to develop a comparison between the potential fluid candidates. This geometry provides the highest wick permeability in a non-screen wick candidate. Wick parameters and heat-pipe performance that result from this decision is listed in Table 3 for each candidate fluid. Clearly, ammonia stands out from the rest, which is consistent with its high Figure of Merit (FOM) listed in Table 1.

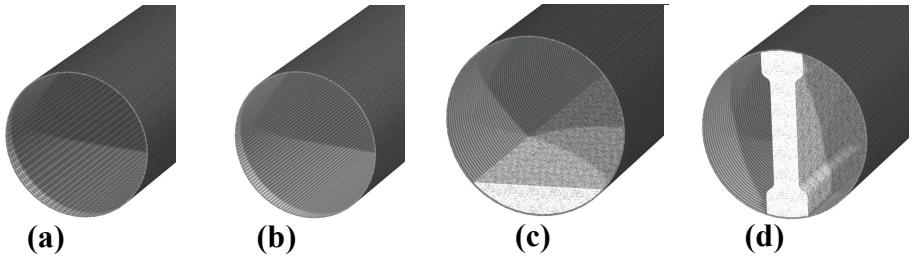

Figure 7: Sketch of heat-pipe wick structures. Wicks are (a) screen wick, (b) axial groove, (c) combination slab and circumferential grooves, (d) slab wick/groove wick with a slab that spans the vapor region.

If we had chosen a *screen* wick, it would not pose a performance limitation[8], but rather a material choice complication. Screen wicks are very porous, but the material choice is generally limited to stainless steel. We have had difficulty finding fine mesh screens in beryllium, which would resolve this issue. Our approach to limiting the material issue in the groove wick is use a very thin metallic coating on the interior of the heat pipe composite wall, which will be discussed next.

[8] The screen wick in effect makes the option for the low pressure Methanol practical.

Table 3: Heat Pipe Performance for Various Fluids

Description/Fluid	NH_3	CH_3OH	C_4H_{10}	R12	C_3F_8	C_4F_{10}
Fluid Conditions						
Saturation Pressure-bar	**2.9**	**0.021**	**1.08**	**2.2**	**2.9**	**0.73**
Temperature-°C	**-10**	**-10**	**-10**	**-10**	**-10**	**-10**
Groove Wick Dimensions						
Number of Grooves	**24**	**32**	**31**	**25**	**47**	**63**
Vapor Core Diameter-mm	**6**	**7**	**6**	**4**	**6**	**6**
Width-mm	**0.4**	**0.33**	**0.3**	**0.25**	**0.2**	**0.15**
Depth-mm	**1.0**					
Wick Performance	**L=400mm, Power=55W**					
Capillary Limit-Watts	**123**	**32**	**19**	**13**	**9**	**5**
Sonic Limit-Watts	**14490**	**180**	**2782**	**1578**	**3704**	**1036**
Boiling Limit-Watts	**478**	**4603**	**192**	**14**	**20**	**80**
Entrainment Limit-Watts	**452**	**56**	**97**	**38**	**78**	**50**

1.1.3 Carbon-Carbon Heat-pipe Inner Metallic Coatings

Allcomp specializes in carbon-carbon products that have found application in ATLAS [4,5], in both the SCT and the Pixel Detector. Recent Allcomp C-C development has focused on C-C wall structures for heat-pipe applications. Allcomp's innovation has been to explore the option of combining a high thermal conductivity C-C wall structure with an ultra-thin metallic coating for an interior hermetic seal. A carbonizable structure with a high temperature coating is directed at high temperature heat-pipe applications. The coatings can be a high temperature metallic or a ceramic, e.g., SiC.

The proof-of-principle tests in sealing have been done, however, *the challenge* is to configure, integrate, and demonstrate a wick suited to high energy physics applications. Our goal for the C-C tube, internal wick and module support is <0.5% X_o. By utilizing all carbon in its construction, exclusive of the thin coating, we hope to achieve this goal.

Figure 8 depicts a photograph of the basic shell structure being produced at Allcomp. The shells produced to date are much thicker than we desire. Our goal is for a tube wall thickness of no more than 0.3mm. Initially, we will prepare a preliminary design of a typical pixel barrel with the heat-pipe/stave concept fully integrated. Based on FEA, we will determine what minimum wall can be used that still satisfies the overall installed stiffness.

Figure 8: Photograph of a Carbon-Carbon composite tube under development for a heat-pipe application. 50 □m layers of nickel and copper used to effect vacuum seal on interior of tube.

We have reviewed potential candidate materials with regard to their physical constants, density (g/cc), unit radiation length (g/cm^2), and effective radiation length (cm). One will find that C-C is second only to Beryllium in radiation length, making it an ideal choice for particle detectors. However, the challenge becomes in adapting thin internal coatings to the C-C outer liner that do not degrade its % X_o. In this regard, aluminum would be a reasonable choice, with a radiation length similar to silicon. A copper/nickel coating thickness is severely limited by radiation length considerations. To utilize this combination, we must confine our use of this material to a very thin coating (s), without a radiation length penalty greater than Al.

Proposed Approach for New Detectors

The approach being taken in present day pixel detector concepts needs to be re-visited if the full potential of precision tracking is to be realized. Through our planned effort, a completely fresh approach will be taken to solving the serious issues associated with pixel detector cooling and support. It is our strong belief that a hybrid cooling system, heat-extraction with passive heat-pipes and heat removal with forced convective coolant, is needed to effectively reduce structural and non-structural mass.

A carbon-carbon heat-pipe derived from this technical effort will offer a means of addressing very high, heat-flux electronic chip applications with minimum chip thermal stress. Presently, the material thermal expansion mismatch between silicon and metallic heat spreaders are causing severe stress problems, particularly in laser-diode applications. A C-C heat-pipe would reduce the thermal expansion mismatch by ten fold.

The objective of our investigation is to demonstrate the performance advantages of a C-C heat-pipe, offering new possibilities in cooling and structural stability in HEP applications. Aspects of this concept can be demonstrated effectively by using a major element taken from ATLAS Pixel Detector, for example one-barrel layer. A test of this magnitude will conclusively demonstrate:

a. Advanced thermal performance features of a C-C heat-pipe
b. Thermal stability of a large scale, low-mass structure
c. Low thermal strains afforded by nearly matched material CTE's

d. Heat rejection of a passive heat-pipe concept to an evaporative cooling system, using highly conductive materials and flow geometry enhancements for maximizing evaporative heat transfer coefficient

A conceptual layout of the proposed C-C heat-pipe integrated with the ATLAS Pixel Detector Barrel has been prepared to illustrate how one improve the structural and cooling aspects (reduce $\%X_o$). The suggested approach dissipates the heat to the C_3F_8 system.

Our concept will replace the ATLAS barrel stave design in its entirety. The present pixel stave structure is composed of three pieces, an OMEGA U-Shaped back support (composite material), a C-C front plate, and an aluminum (Al) cooling tube containing the C_3F_8 evaporative fluid. The Al tube is confined between the OMEGA piece and C-C front plate; the volume surrounding the tube is filled with thermally conductive grease by AI Technology. The thermal grease provides a measure of structural decoupling between the high CTE of the Al tube and the composite parts. In our concept, the 0.2mm wall Al tube is replaced with a C-C cooling heat-pipe that has greater stiffness, thus eliminating the OMEGA piece and grease. For example, a nominal 6mm heat-pipe with a 0.25mm C-C wall and a 50□m Al liner, has roughly the same radiation length as the 0.2mm Al tube [6], but it would be 6.2 times stiffer than the tube. Elimination of the OEMGA piece and the CGL7018 thermally conductive grease is a savings of 0.16% in X_o.

The continuous C-C module top carrier in ATLAS would be replaced with individual composite heat spreaders. The new stave geometry is shown in Figure 9. To provide detector overlap in the axial direction, the top C-C plate in ATLAS is shingled, with a minimum thickness of 0.4mm increasing to 1.6mm, with an average radiation length [6] of 0.47%. In the proposed design, we use a step-up and step-down pattern to overlap. In implementing this concept, we would recommend a thermal heat spreader thickness not exceeding 0.5mm, a potential radiation length savings of 0.2%. This comparative quick appraisal indicates that these X_o savings amount to 0.36% in the stave alone.

In our earlier discussion, we indicated that it might be possible to eliminate the shell support for the staves, by adopting a configuration similar to the CMS design. This objective would bring the total savings per layer to > 0.5%.

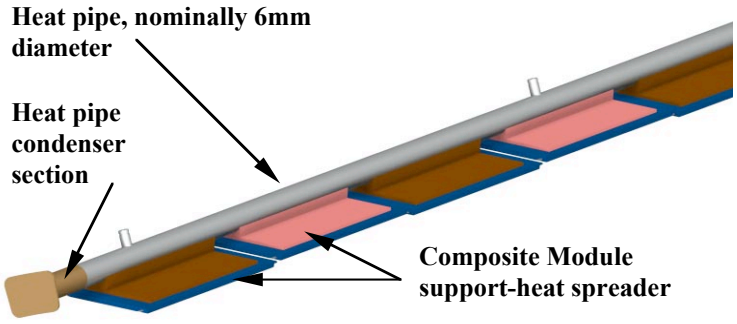

Figure 9: Illustration of a proposed stave concept using a heat-pipe for cooling and support. The modules are supported individually with a composite sandwich of C-C material, with a highly thermally conductive core of pyrolytic graphite.

To complete the transformation to a C-C heat-pipe concept, a design approach for the removing the heat from the heat-pipe condenser section is needed. Although, a concept of this aspect needs to be investigated in detail, we illustrate two suggested approaches here, Figure 10 and Figure 11. The condensing section of the C-C heat-pipe will be placed in the 40mm region between the end of the present stave and the support end cone for the barrel region. In the first approach (Figure 10), we propose that heat be transferred to a simple tube/plate C_3F_8 heat exchanger (HE). The fluid passes through the tubes as a two-phase fluid (-30°C), as presently occurs in the ATLAS stave, and exits the manifold mostly vapor. However, in this case the C_3F_8 fluid picks up the heat from many heat-pipes. The arc length of the tube/plate HE is of choice, including using two parallel tubes for increased reliability. The plate extracts heat from the heat-pipes in a barrel half, e.g., _ of the circumference for a clamshell structure. If one so chooses, multiple C_3F_8 tubes, sized appropriately, can be used for this split arrangement with any one tube being able to remove the total heat. In this manner, full system redundancy in the cooling system can be provided. Because the C_3F_8 has a high saturation pressure and density at -30°C, there is ample hydraulic energy for the vapor return to the C_3F_8 compressor.

We have made a first approximation to the effective CTE for the composite heat-pipe tube. The C-C heat-pipe with Al liner would have a CTE of –0.038ppm/K and the same geometry with the Ni/Cu liner would have –0.007ppm/K. For all practical purposes, their CTE's are zero. A shell support constructed from YSH50 graphite fibers, 58% fiber fraction quasi-isotropic fiber lay up, would also be near zero CTE. Thus, the shell and heat-pipe are well matched, eliminating the need for kinematic supports for the heat-pipe assembly. This overcomes one of the inherent problems found in the ATLAS design.

There is however, the issue of dissimilar CTE's between the pixel module and heat spreader support. CGL7018 AI Technology's low-stress, thermally conductive paste could be used to join the module to the heat spreader. Later we will work out a low strain attachment of the heat spreader to the C-C heat-pipe. Our experience with C-C and resin matrix composites will be helpful in this task.

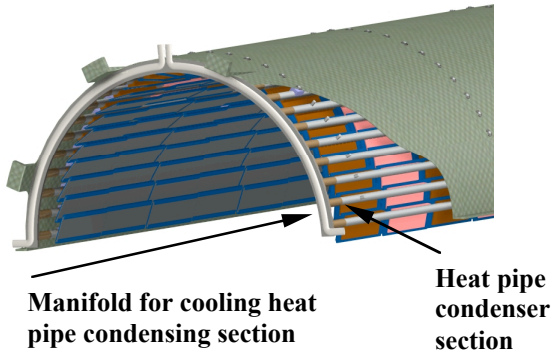

Figure 10: Illustration depicting connection of the cooling system manifold to the heat-pipe condenser section.

The second approach uses a C_3F_8 cooling manifold, which contains fins for enhancing the heat exchange. The manifold slides on the end of the tubes as a unit. The manifold will be either

bonded with a demountable adhesive, or the low shear modulus CGL7018 thermally conductive, semi-rigid paste material.

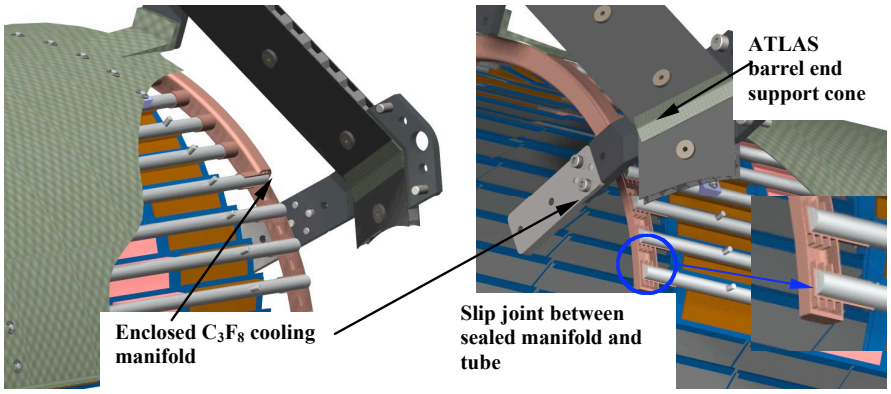

Figure 11: Concept of evaporative coolant manifold to remove heat from the heat-pipe tube ends.

In both approaches, we will concentrate on minimizing the mass of the heat exchange components. One will notice we have eliminated the massive PEEK end rings used in the present ATLAS shell used for strain relief of the services. We have also dramatically reduced the number of cooling inlet and exit lines in the detector volume. Note also that we cool the shell simultaneously with the new stave concept. This is intended to eliminate thermal strains during cool-down.

References

1. ATLAS Inner Detector Technical Design Report Volume 2, CERN/LHCC/97-17, ATLAS TDR 5, dated 30 April 1997.
2. Private communication with Marco Olcese, projected radiation length budget for ATLAS Pixel Detector structures, Figure 3.
3. M. Olcese, "*Pixel Detector Local Supports: Carbon Monolithic Stave*", dated 22 October 1998, presented at the CERN ATLAS Inner Detector Engineering Review.
4. Ultra-Lightweight Carbon-Carbon Cooling Structure for Pixel Detector and Silicon Strip Detectors, Department of Energy Research, Small Business Innovative Research (SBIR) Grant DE-FG03-97ER82397
5. Low Cost Support Structures with New Advanced Composite Materials Tailored for Ultra-Stable Particle Tracking Detectors, Department of Energy Research, Small Business Innovative Research (SBIR) Grant DE-FG03-99ER82801.
6. S. Cuneo, I.N.F.N. Genoa, ATLAS Pixel Mechanics: June 15, 2000, "Baseline Stave Report"